Fourth Term Report: Mathematical Modelling of Manufacturing Processes for Control

Jeremy Minton
Supervisor: Ed Brambley

November 9, 2014

1 Introduction

For much of human history, manufacturing relied on skilled artisans to hand produce each item. The industrial revolution introduced machine-based manufacturing and then developments in mass production lead to each item's creation being divided into many small processes for automation or greater mastery by a labourer. Machines are now able to accomplish nearly every step of a manufacturing process.

Recent market trends for customisability and manufacturing management strategies, like just-in-time manufacturing, has increased the demand for highly automated yet flexible processes. Computer numerical control (CNC) machines have met that demand and are now common place in additive and subtractive manufacturing: milling and 3-d printing as respective examples. With additional sensing and closed loop control, or real time optimisation, CNC is also able to adapt for material imperfections and machine wear to achieve higher quality and consistency.

Development in forming automation has not followed suite due to a dependence on part specific tooling. Consequently, most forming processes remain largely open loop, relying on many repetitions to find an optimal operating condition or even human controlled tooling. This may be sufficient for mass produced items but is unable to meet the demand of flexibility and tightening quality margins.

A successful control systems would depend on an understanding of the ongoing process in the form of a predictive model that can be computed in real time or faster. Current design processes using finite element models are computationally too slow, so many empirical or ad-hoc models are used instead. For example, Orowan's model[Orowan, 1943] for rolling, which will be described in section 2.

Using a more mathematically rigorous approach we hope to develop faster solutions that are sufficiently accurate for control systems and help to make CNC forming a reality. This systematic approach will also provide insight into the underlying dynamics of forming to improve modelling assumptions and inform processes design decisions.

Collaborators in CUED are experimentally investigating control of a range of processes such as ring rolling and spinning. Ring rolling reduces the thickness of a ring shaped workpiece by rotating through a pair of rolls called the mandrel and work roll. A second pair of rolls, called the axial rolls, can also be used to reduce the height of the workpiece, a squeezing out of the page in fig. 1. Depending on the operation parameters and use of axial rolls, the workpiece diameter or height can be enlarged as the thickness is reduced. The ongoing investigation is to control this cross sectional change while applying finer rolls to produce cross-sections more complex than rectangles.

Spinning deforms a circular plate by rotating it while deforming it with a roller as indicated by fig. 2. The roll indicated would make multiple passes along the radial length of the workpiece to incrementally deform the workpiece towards the final shape. This deformation is typically onto an axi-symmetric mandrel that defines the final shape so that the workpiece can be pressed firmly onto it. The current investigation is to replace the mandrel with additional rollers such that each unique product shape does not require the production of a mandrel but rather a set of tool paths for a collection of independently moving rollers.

There is also a project to construct an experimental flat-sheet rolling machine, much like ring rolling but passing a flat sheet through a pair of rolls as opposed to a ring. The machine is being designed to also apply bending moments on the sheet moving into and out of the roll gap.

To support the research to be performed with this machine, and as a means of developing an understanding of the field by building on existing literature, my enquiry has focused on flat sheet rolling thus far.

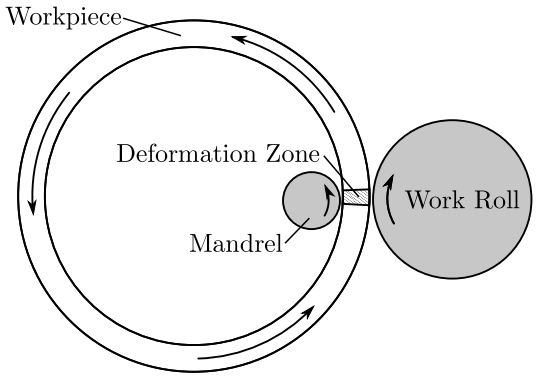

Figure 1: A schematic of the ring rolling process.

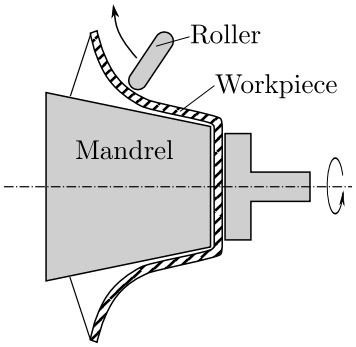

Figure 2: A schematic of the spinning process.

1.1 A primer to rolling

Rolling is the process of reducing the thickness of a flat metal sheet by passing it through two metal rolls. Rolling exists in many different regimes but is generally classed into hot and cold rolling. Hot rolling occurs above the metals recrystallisation point to prevent work hardening. This process is used in rough rolling to reduce large pieces, such as cast products, in to a size appropriate for subsequent stages of manufacture. Some finished products produced with hot rolling are sheet metal, I-beams, vehicle frames, building materials and other items with simple cross-sections. Cold rolling occurs below the metals recrystallisation point so strain hardening is a by-product. This can be up to 20% increase in strength with a 50% reduction in material thickness. With this limit on reduction, and an improved surface finish, cold rolling encompasses the last rolling passes for a workpiece and so the workpiece is typically much thinner. Typical products are metal furniture, computer hardware, metal drums and thinner sheet metal.

Although some processes require variations, such as four-high cold rolling mills, functionally rolling consists of material passing through to turning rolls that reduce the thickness of the material. Figure 3 is a diagram of this idealised process.

It is worth noting some key features of the process and introducing some terminology. The roll half thickness, $\hat{h}_0$; the roll radius, $\hat{R}$; and the entrance velocity, $\hat{u}_0$ are all marked. The roll bite is the shaded region with the roll bite length marked as $\hat{l}$. Finally, the half gauge, $\Delta\hat{h}$, is marked, which is distinct from reduction, $r = \Delta\hat{h}/\hat{h}_0$, or the change in thickness as a fraction of the original thickness. This distinction will not be significant as these become equivalent in most non-dimensionalisations.

Variables denoted with a hat, like the ones here, are taken to be dimensional. This is a convention used throughout this document.

Rolling can be considered a generalised extrusion process; where the boundaries of an extrusion die are stationary, the rolls of a rolling mill will rotate at some speed. Considering conservation of mass, it is clear that the material moves faster as it passes through the roll gap. These two facts result in a neutral point: a point where the material of the workpiece travels at the same speed as the roll. This is depicted in fig. 4 and marked as $\hat{x}_n$.

The position of the neutral point will vary depending on the end forces of the workpiece. The special

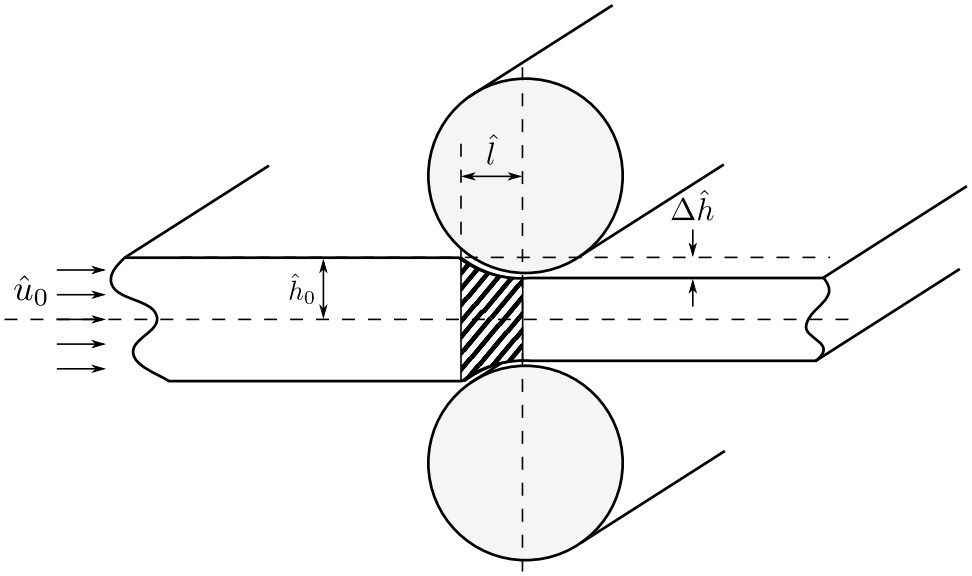

Figure 3: A two-dimensional schematic of rolling.

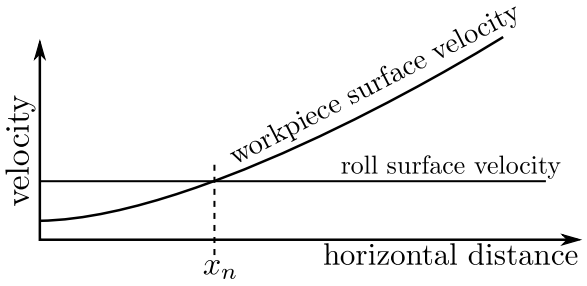

Figure 4: A characteristic plot of the tangential boundary velocity of the workpiece.

case of extrusion, where the neutral point moves past the roll bite entrance, requires some large external pressure driving the workpiece through the roll bite. Generally a combination of end forces and friction move the sheet through the roll gap.

Assuming there is no counter flow at the workpiece edges, this differing in speed will result in material slipping along the contact faces and hence friction acts to squeeze the workpiece towards the neutral point.

This compression builds pressure from both ends to a maximum at the neutral point. This phenomena is often referred to as the pressure hill. It is established by experiment and borne out in all rolling models including those presented here.

2 Review of Rolling Literature

Modelling of rolling began in early twentieth century Germany with notable publications including Siebel [1924], Siebel and Pomp [1927], Karman [1925] and Nadai [1931]. These all present variations of a slab model: a model neglecting shear so each section of material can be vertically solved as a compression problem. Some experimental results would indicate towards this assumption, however, there is no rigorous basis for it and it's application in a wide set of regimes is largely unsupported. Despite this, slab models are still being developed and extended to new areas; areas such as asymmetric rolling where shear is likely to become more significant. This will be returned to below.

The next major contribution came from Orowan [1943] in which an approximate model is presented that incorporates shear. Horizontal and vertical force balances are closed by assuming that, locally, the solution can be approximated by Nadai's compressing wedge solution [Nadai, 1931]. This is achieved by considering the section of material contained within the two lines A-A' in fig. 5. Assuming this region is in dynamic equilibrium then the forces on the dashed line must equal those on the solid line. Then deforming the dashed line to be the circumference of a circle perpendicularly intersecting the rolls and

approximating the rolls by flat tangential surfaces a wedge is created. Applying a wedge solution to this section closes the force balance for each slab of material.

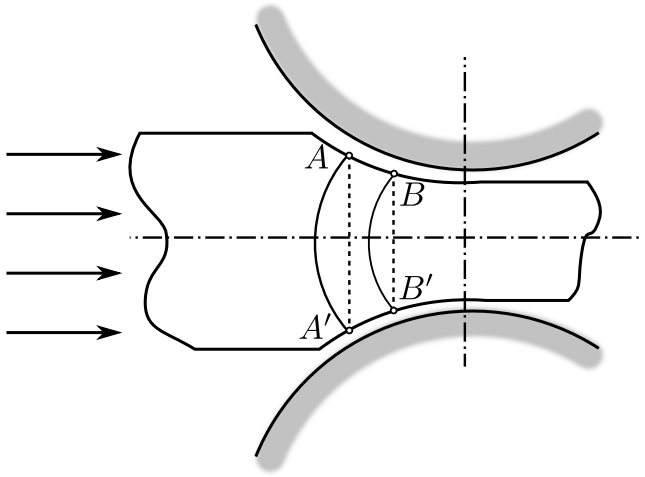

Figure 5: Diagram indicating the deformation to the elemental slab made by Orowan to apply the compressing wedge solution.

Despite Orowan's claims to eliminate ad-hoc assumptions from the analysis, the validity of this assumption is questionable for two reasons. Firstly, the approximation of the region to a wedge has not been established in any way and, secondly, the compressing wedge solution, although exact, can only be found for material moving toward the wedge apex limiting it's correctness to the inlet side of the neutral point. Despite these inaccuracies, this solution has been generally adopted as a benchmark and is widely used by industry, although with empirically fitted parameters.

Some developments since then include Orowan and Pascoe [1946], Bland and Ford [1948b] and Bland and Ford [1948a] which extend Orowan's original work in areas such as incorporating tensions or making additional assumptions to simplify the calculation process.

Slip-line theory has also been utilised in two publications: Alexander [1955] and Collins [1969]. These develop sticking and slipping models respectively although the latter is limited to a qualitative investigation due to the complexity of the fields. Two additional slip-line methods for asymmetric rolling are discussed in the section below.

Hartley et al. [1989] provides the first review of rolling which predominantly covers these classical models as well as experimentation and some early finite element simulation.

Many numerical studies have been performed since they began in 1972 with Alexander [1972]. Notably, Venter and Abd-Rabbo [1980] and Venter and Adb-Rabbo [1980] develop numerical implementations of the Orowan [1943] solution. Finite element simulations have since become very popular and several reviews exist including Montmitonnet and Buessler [1991] and Montmitonnet [2006], in which 34 and 25 publications of numerical studies have been reviewed respectively. It is, in fact, included as an example problem in the commercial finite element package, *ABAQUS*, 'Example Problems Manual' [Dassault Systemes, 2012]. Despite this ubiquity the result processing remains slow, too slow for control, and the quantitative knowledge from these investigations is difficult to transfer; the process of constructing and solving these simulations is often repeated for nearly identical set-ups in independent studies.

2.1 Asymptotic Methods

More recently, asymptotic methods have been applied to solve a complete set of governing equations in the limit of a small aspect ratio: thin sheets and large rollers. It was first utilised in metal forming, specifically conical extrusion, in 1987 by Johnson. Having transferred these techniques from modelling creep in glaciers, he considers a pseudo-steady-state conical extrusion of a power-law rate hardening elasto-plastic with Coulomb friction. The asymptotic limit used is quite elegant in that it considers deviation from a 'plug-like' flow making the solution valid for either low friction or shallow dies. One or both of these assumptions form the basis of all following asymptotic methods in forming. One other

publication could be found that examines solid metal extrusion with asymptotics, Govindarajan and Aravas [1991], and it considers small reduction rate extrusion before adding metal porosity.

Johnson is a named author on numerous publications that apply the same techniques to sheet rolling. The first of these is Smet and Johnson [1989], followed three years later by Johnson and Smelser [1992]. The former applies an almost identical process to that in Johnson [1987] while also neglecting elasticity. The major distinctions from extrusion being in the geometry and direction of friction: opposite direction either side of the neutral point. The latter makes a number of simplifications to the former to progress further to a closed form solution; a rigid-plastic material with yield stress as an arbitrary function is used and the magnitude of surface friction is set to be a constant fraction of the yield stress.

Although yielding single integral solutions, these assumptions may fail to accurately capture the physics of the problem, particularly the friction model. This motivated a similar formulation in Domanti and McElwain [1995], who re-introduces the more commonly used Coulomb friction, while assuming the ratio of maximum pressure to yield stress is large and the reduction is small. The first of these requires compressive end conditions and the latter, due to the coupling between reduction, roll bite length and sheet thickness, restricts the valid geometry. Finally, the most comprehensive two-dimensional formulation to date is presented in Cherukuri et al. [1997]. Using a relative-slip friction model and strain-rate dependent constitutive equations, the governing equations are solved to ODEs, assuming only a small aspect ratio. This is repeated for small, medium and large friction and no-slip conditions.

Asymptotic approaches to three dimensional effects and spread are Johnson [1991] and Domanti et al. [1994]. The former has a rare comparison to finite element simulations and experimental results. Asymptotic analysis has also been used for stability analysis of 'chatter' in Johnson [1994a]; a multiple scales analysis of work roll heat transfer in Johnson and Keanini [1998]; and a model for roller deformation in Langlands and McElwain [2002]. Other considerations include surface finish, heating and residual stresses. A review of modelling methods applied to rolling is presented in Domanti and McElwain [1998] although no comparison of results is made.

2.2 Asymmetric Rolling

Asymmetric rolling, when not unintentional, exploits unequal drive, friction or size of the rolls to reduce total force and torque, improve surface finish or improve strain hardening. The challenge, however, is that asymmetry results in sheet curvature which can be undesirable.

Experimentation has been used to quantify roll force and torque for a range of geometries and materials [Siebel, 1941, Sachs and Klinger, 1947]. A variety of techniques have also been used to investigate other properties such as contact stress distributions and workpiece curvature [Johnson and Needham, 1966, Buxton and Browning, 1972, Ghobrial, 1989].

Analytical work has included a range of solutions, most popular is modifying slab models [Chekmarev and Nefedov, 1956, Kennedy and Slamar, 1958, Sauer and Pawelski, 1987] which has seen incremental development to include greater asymmetry and curvature predictions [Mischke, 1996, Hwang and Tzou, 1996, Salimi and Sassani, 2002]. Alternatives also include the upperbound method [Pan and Sansome, 1982, Kiuchi and Hsiang, 1986] and slipline methods [Dewhurst et al., 1974, Collins and Dewhurst, 1975], both of which are able to predict curvature.

Finite element simulations have also been applied to provide detailed solution information for more general configurations. Most studies focus on curvature prediction and roll force distributions [Shivpuri et al., 1988, Richelsen, 1997, Knight et al., 2005].

Asymptotic analysis has only been applied to asymmetric rolling in Johnson [1994b] where an asymmetric friction and roll speed were considered in a friction factor model, that is the surface shear is equal to a constant factor of shear flow. Asymmetric friction was investigated by changing each rolls friction coefficient and asymmetric roll speed was modelled by having two independent neutral points and a region of cross shear between them. Roll geometry was also discussed briefly but dismissed as being able to be incorporated into the friction coefficient. Experimental evidence that shows the direction of curvature in asymmetric rolling is dependent on geometry suggests this is approximation is insufficient [Collins and Dewhurst, 1975].

3 Governing Equations

Considering an elemental unit of material that is confined by plane strain - that is independence, through zero strain, in the z direction - horizontal and vertical force balances are immediately obvious,

$$-\frac{\partial \hat{p}}{\partial \hat{x}} + \frac{\partial \hat{s}_{xx}}{\partial \hat{x}} + \frac{\partial \hat{s}_{xy}}{\partial \hat{y}} = 0,$$
$$\text{and} \quad -\frac{\partial \hat{p}}{\partial \hat{y}} + \frac{\partial \hat{s}_{yy}}{\partial \hat{y}} + \frac{\partial \hat{s}_{xy}}{\partial \hat{x}} = 0.$$

where $\hat{p}$ is the pressure and $\hat{s}_{ij}$ is the ij^{th} element of the deviatoric stress tensor.

At least one more equation is required to close this system and completely determine the state of stress although, typically, at least four more exist as a material flow rule and yield condition. Many flow rules exist to describe different materials but the common Prandtl-Reuss equations will be used here,

$$\frac{\partial \hat{u}}{\partial \hat{x}} = \hat{\lambda}\hat{s}_{xx},$$
$$\frac{\partial \hat{v}}{\partial \hat{y}} = \hat{\lambda}\hat{s}_{yy},$$
$$\text{and} \quad \frac{\partial \hat{u}}{\partial \hat{y}} + \frac{\partial \hat{v}}{\partial \hat{x}} = 2\hat{\lambda}\hat{s}_{xy},$$

where $\hat{\lambda}$ is the time differential of the flow parameter. This additional variable is introduced to ensure both compatibility and the yield condition can be met. Again, many yield conditions exist but the commonly used von Mises yield condition has been selected here. It is assumed that the entire roll bite is undergoing plastic deformation and hence is at yield giving the equality

$$\hat{s}_{xx}^2 + \hat{s}_{yy}^2 + 2\hat{s}_{xy}^2 = 2\hat{k}^2.$$

where $\hat{k}$ is the yield stress in shear, taken to be a constant.

The selection of flow rule and yield condition are commonly used models and in this form describe a rigid-perfectly plastic material. There are numerous more models that have been developed to describe additional phenomena or specific characteristics of certain materials. These are discussed later in this section and again in section 6 in the context of further investigations to build on this existing model.

3.1 Boundary Conditions

The velocity on the roll surface is attained from considering the incompressibility condition,

$$\hat{v}(\hat{x}, \hat{h}_t(\hat{x})) = \hat{u}(\hat{x}, \hat{h}_t(\hat{x}))\frac{d\hat{h}_t}{d\hat{x}}.$$

Stress conditions are found by considering horizontal and vertical equilibrium on a boundary volume element,

$$\hat{\sigma}_{xx}\frac{d\hat{h}_t}{d\hat{x}} - \hat{s}_{xy} + \hat{\tau}_t - \hat{s}_t\frac{d\hat{h}_t}{d\hat{x}} = 0$$
$$\hat{\sigma}_{yy} - \hat{s}_{xy}\frac{d\hat{h}_t}{d\hat{x}} - \hat{s}_t - \hat{\tau}_t\frac{d\hat{h}_t}{d\hat{x}} = 0.$$

where $\hat{\sigma}_{ii} = -\hat{p} + \hat{S_{ii}}$, $\hat{\tau}$ is the interfacial traction stress and $\hat{s}$ is the interfacial normal stress. Apply plane stress, $\hat{s}_{xx} = -\hat{s}_{yy}$, to the previous result for

$$\hat{s}_{xy} = \hat{\tau}_t\left(1 + \left(\frac{d\hat{h}_t}{d\hat{x}}\right)^2\right) - 2\hat{s}_{xx}\frac{d\hat{h}_t}{d\hat{x}} + \hat{s}_{xy}\left(\frac{d\hat{h}_t}{d\hat{x}}\right)^2$$

This is closed with a friction model; like material models a large range of friction models exist.

3.1.1 Coulomb Friction

Coulomb friction is a widely used friction model and has been applied to static and slipping friction, although coefficient values are often very different. It is developed on the assumption that the traction force is proportional to the normal pressure,

$$\hat{\boldsymbol{\tau}} = \mu \hat{\boldsymbol{\sigma}} \cdot \hat{\mathbf{n}} \frac{\Delta \hat{\mathbf{u}}}{|\Delta \hat{\mathbf{u}}|}.$$

where $\Delta \mathbf{u}$ is the relative slip velocity of the plastic material past the surface and μ is a constant friction coefficient.

3.1.2 Relative-Slip

Relative-slip friction is a slipping model as it defines the traction force as proportional to the velocity difference between the surfaces in contact,

$$\hat{\boldsymbol{\tau}} = \hat{\kappa} \Delta \hat{\mathbf{u}}.$$

where $\hat{\kappa}$ is a constant friction coefficient.

3.1.3 Assorted Others

An assortment of other models that have been identified in literature are also included for discussion.

Friction Factor The friction factor model appears to be a large simplification, often used to make a problem more tractable. It assumes that the traction force is constant at some fraction of the yield stress,

$$\hat{\boldsymbol{\tau}} = c\hat{k} \frac{\Delta \hat{\mathbf{u}}}{|\Delta \hat{\mathbf{u}}|}.$$

where c is a constant friction factor.

No-slip The no-slip condition assumes that the traction is sufficiently high to ensure the materials stick. In terms of velocities it is

$$\hat{\mathbf{u}} = \hat{\mathbf{U}},$$

where $\hat{\mathbf{U}}$ is the roll velocity. For rigid perfectly-plastic, and other, materials this will leave the stresses undetermined and so the associated stress condition is a friction factor model where $c = 1$.

Transitional Models As the traction exceeds the material yield, the friction will transition from a slipping to a no-slip model. Some solutions are able to capture this behaviour, such as Orowan [1943].

Similarly, some models try to combine Coulomb and relative-slip friction with some transition region. Experimentally there is evidence that the former performs well for static and low relative velocity differences where the latter is better for higher relative velocities.

One such example of this is a model developed in Karabin and Smelser [1990]:

$$\begin{aligned} \hat{\boldsymbol{\tau}} &= |\hat{\boldsymbol{\tau}}| \frac{\Delta \hat{\mathbf{u}}}{|\Delta \hat{\mathbf{u}}|} \\ \text{where} \quad |\hat{\boldsymbol{\tau}}| &= \min\left(\mu \psi \hat{s}, \hat{k}\right) \\ \text{and} \quad \psi &= \min\left(\frac{|\Delta \mathbf{u}|}{\Delta_v}, 1\right) \end{aligned}$$

where μ and Δ_v are both constants and note that ψ is defined with a nondimensionalised slip velocity. Effectively this formulation will behave like relative slip at low slip speeds, when $\psi < 1$, then transition to a Coulomb model at higher speeds, $\psi = 1$ makes $|\hat{\boldsymbol{\tau}}| = \mu \hat{s}$, before transitioning to a sticking model to not exceed the yield condition, $|\hat{\boldsymbol{\tau}}| = \hat{k}$.

4 Symmetric Rolling

The models presented in this section have not been explicitly presented in literature, however, they are only variations in modelling assumptions from the four publications of asymptotic modelling of two-dimensional symmetric rolling discussed in section 2.1. Although this work is in part filling in the gaps left in literature some interesting insights arise about limitations of certain assumptions. This

suggests at the need for additional phenomena to be modelled in order to achieve complete consistency. This section begins by non-dimensionalising the equations presented in the previous section with some discussion about the choice of scaling. One of several choices of scaling is selected to present the solution method. This is completed for a general friction model before both Coulomb and relative-slip models are applied. Some results from these models as well as a higher friction scaling solution are presented with a discussion of their limitations and challenges which may go some to explain the selection of models used in the existing literature.

4.1 Nondimensionalisation

It is worth first noting, again, that dimensional quantities are denoted with a hat and non-dimensional quantities without.

Defining δ as the ratio of vertical to horizontal characteristic length scales, input half thickness and roll bite length respectively so $\delta = \hat{h}_0/\hat{l}$, indicates a number of obvious scalings. This is the small parameter that featured often in previous asymptotic studies of rolling and extrusion. It is crucial to attaining a separation of directional derivatives, essential to arriving at a closed form solution.

The first is velocity; the horizontal velocity is scaled by some characteristic velocity, $\hat{u} = u\hat{u}_0$, taken here as the input velocity. This can can ultimately be chosen to satisfy the roller speeds if the problem is defined as such. The vertical velocity is taken to balance the horizontal velocity in the no-penetration boundary conditions, hence scaling $\hat{v} = v\delta\hat{u}_0$.

The stress scalings are less obvious as some constraints exist yet there remains freedom to decide some relative sizes. Begin by defining characteristic shear, deviatoric longitudinal stress and pressure, $\hat{ta}u_0$, $\hat{s}_0$ and $\hat{p}_0$. Now consider the yield condition. This suggests the larger (or both if similar magnitude) of the deviatoric stresses could be scaled by the yield stress k.

Balancing the derivatives in each direction of the horizontal equilibrium requires $\hat{\tau}_0 = \delta\max(\hat{s}_0, \hat{p}_0)$ although solving in the case where $\hat{s}_0 > \hat{p}_0$ leads to an inconsistency: pressure jumps an order. This indicates that the more correct balanced is between pressure and shear stress hence $\hat{\tau}_0 = \delta\hat{p}_0$. Finally, define $\bar{\beta}$ as the ratio of characteristic deviatoric shear to longitudinal stresses, $\hat{\tau}_0/\hat{s}_0$, and it is possible then to enumerate three possibilities based on the magnitude of $\bar{\beta}$.
In ascending order, if $\bar{\beta} = O(\delta)$ then

$$\hat{s}_0 = \hat{k}, \qquad \hat{\tau}_0 = \bar{\beta}\hat{k} \quad \text{and} \qquad \hat{p}_0 = \frac{\bar{\beta}}{\delta}\hat{k}.$$

If $\bar{\beta} = O(1)$ then

$$\hat{s}_0 = \hat{k}, \qquad \hat{\tau}_0 = \bar{\beta}\hat{k} \quad \text{and} \qquad \hat{p}_0 = \frac{\bar{\beta}}{\delta}\hat{k}.$$

But, if $\bar{\beta} = O(\delta^{-1})$ then

$$\hat{s}_0 = \frac{\hat{k}}{\bar{\beta}}, \qquad \hat{\tau}_0 = \hat{k} \quad \text{and} \qquad \hat{p}_0 = \frac{\hat{k}}{\delta}.$$

As it may be obvious by it's definition, $\bar{\beta}$ is some measure of the size of friction. In it's most elegant case it maps to the Coulomb friction coefficient but may depend on other parameters, such as velocities in the relative-slip model. A selection of these regimes have been made implicitly in the previous asymptotic rolling literature. Smet and Johnson [1989], Johnson and Smelser [1992] both use the middle friction regime and Domanti and McElwain [1995] assumes the friction is small yet the pressure is large which contradicts these scalings. To achieve this compressive end conditions are required to raise the pressure in the roll gap - a point not mentioned in the publication. This choice was made explicitly in Cherukuri et al. [1997] where all three were addressed. The reason for the limited selection may be due to some of these regimes being incompatible with certain material or friction models. This point is discussed in greater detail in section 4.5.

The final scaling to decide is the flow parameter which is chosen such the horizontal flow equation balances at leading order, hence $\hat{\lambda} = \frac{\hat{u}_0}{\hat{k}\hat{l}}\lambda$ or $\hat{\lambda} = \frac{\hat{u}_0\bar{\beta}}{\hat{k}\hat{l}}\lambda$.

As this solution process becomes both expansive and repetitive it will be presented only once for the case where $\bar{\beta} = O(\delta)$ and other regimes will be illustrated through making comparison to this solution.

For convenience, let $\beta = \bar{\beta}/\delta = O(1)$.

This gives the governing equations for force equilibrium,

$$-\beta\frac{\partial p}{\partial x}+\frac{\partial s_{xx}}{\partial x}+\beta\frac{\partial s_{xy}}{\partial y}=0, \tag{1}$$

$$-\beta\frac{\partial p}{\partial y}+\frac{\partial s_{yy}}{\partial y}+\beta\delta^2\frac{\partial s_{xy}}{\partial x}=0; \tag{2}$$

flow,

$$\frac{\partial u}{\partial x}=\lambda s_{xx}, \tag{3}$$

$$\frac{\partial v}{\partial y}=\lambda s_{yy}, \tag{4}$$

$$\frac{\partial u}{\partial y}+\delta^2\frac{\partial v}{\partial x}=2\delta^2\beta\lambda s_{xy}; \tag{5}$$

incompressibility, or equally in this case, plane strain,

$$\frac{\partial u}{\partial x}+\frac{\partial v}{\partial y}=0; \tag{6}$$

and yield,

$$s_{xx}^2+s_{yy}^2+2\delta^2\beta^2 s_{xy}^2=2. \tag{7}$$

with boundary conditions for velocity,

$$\begin{aligned} v(x,h)&=u(x,h)\frac{dh}{dx}\\ v(x,0)&=0, \end{aligned} \tag{8}$$

and shear,

$$\begin{aligned} s_{xy}(x,h)&=\tau(x)\left(1+\delta^2\left(\frac{dh}{dx}\right)^2\right)-\frac{2}{\beta}\frac{dh}{dx}s_{yy}(x,h(x))+\delta^2 s_{xy}(x,h(x))\left(\frac{dh}{dx}\right)^2\\ s_{xy}(x,0)&=0, \end{aligned} \tag{9}$$

where we approximate the roll as a parabola so that

$$\begin{aligned} h&=1-r(2x-x^2)\\ \text{and}\quad \frac{dh}{dx}&=-2r(1-x). \end{aligned} \tag{10}$$

Taking all parameters as $O(1)$, except δ, these equations are solved for a perfect-plastic, small aspect ratio, plane-strain rolling set up.

4.1.1 Expansion in δ

Taking the aspect ratio, δ, as the small parameter, each dependant variable, v_x, v_y, S_{xx}, S_{yy}, S_{xy}, p and λ, is expanded in typical asymptotic style.

$$a(x,y)=a^{(0)}(x,y)+\delta a^{(1)}(x,y)+\delta^2 a^{(2)}(x,y)+....$$

Substituting these expansions into the governing and then assuming δ is sufficiently small that each power of δ is disparate and can be considered orthogonal. Grouping like terms produces a series of, what is hoped to be, tractable equations that can be progressively solved for an increasingly accurate solution.

4.1.2 Considering $O(1)$ Terms

Begin by determining the leading order velocities; integrating eq. (5) shows that leading order horizontal velocity is a function of x only. Using a conservation argument and mass flow in and out of any vertical slab spanning the roll gap readily produces the result

$$u^{(0)}=\frac{1}{h(x)}. \tag{11}$$

Substituting this into eq. (6) gives an equation for the leading order vertical velocity. After integration and the application of the boundary conditions, eq. (8), the solution is found to be

$$v^{(0)} = \frac{y}{h(x)^2}\frac{dh}{dx} \tag{12}$$

Now the longitudinal deviatoric stresses are determined with eq. (7). Applying plane strain at leading order leaves

$$s_{xx}{}^{(0)} = -s_{yy}{}^{(0)} = 1 \tag{13}$$

where the sign has been chosen to satisfy the compression from the rolls. Choosing the opposite signs would require compression end conditions of greater magnitude than the compression of the rollers.

Diverting momentarily from stresses, rearranging eq. (3) for the flow parameter gives

$$\lambda^{(0)} = \frac{1}{h(x)^2}\frac{dh}{dx} \tag{14}$$

Returning now to shear stress and pressure. These remaining variables are coupled through the horizontal force balance and the choice of friction condition. Fortunately, substituting the result eq. (13) into the vertical force balance, eq. (1), reveals that the leading order pressure is independent of y. This, with eq. (13) substituted again, simplifies this coupling to a pressure derivative balanced by a shear derivative. Integrating in y between the boundary conditions and substituting eq. (9) gives an equation for pressure,

$$\frac{dp^{(0)}}{dx} = \frac{s_{xy}{}^{(0)}(x,h(x))}{h(x)} = \frac{\tau^{(0)}(x)}{h(x)} + \frac{2}{\beta h(x)}\frac{dh}{dx}. \tag{15}$$

This will either be an integral equation for relative-slip friction or an ordinary differential equation for Coulomb friction or something less tractable for more complex boundary conditions.

There will be at least one constant of integration that is yet to be determined. This constant(s) is part of a system that is solved to satisfy the end forces. Ultimately this system comes down to solving for roll velocity, the workpiece velocity - the velocity scaling $\hat{u}_0$ chosen - and the magnitude of pressure - the undetermined coefficient. The position of the neutral point is also determined by this system.

Either by inspection or by an indefinite integral in y it can be determined that leading order shear is linear in y. With both boundary conditions, eq. (9), this is sufficient to determine

$$s_{xy}{}^{(0)} = y\frac{s_{xy}{}^{(0)}(x,h(x))}{h(x)} = y\left(\frac{\tau^{(0)}(x)}{h(x)} + \frac{2}{\beta h(x)}\frac{dh}{dx}\right). \tag{16}$$

4.1.3 Considering $O(\delta)$ Terms

Repeating this process for the next order leads to the first order velocities, flow parameter and longitudinal deviatoric stresses all to be uniquely zero. Both the first order pressure and shear stress will also be zero unless there is some first order frictional effect, given

$$\frac{dp^{(1)}}{dx} = \frac{s_{xy}{}^{(1)}(x,h(x))}{h(x)} = \frac{\tau^{(1)}(x)}{h(x)} \tag{17}$$

$$\text{and} \quad s_{xy}{}^{(1)} = y\frac{s_{xy}{}^{(1)}(x,h(x))}{h(x)} = y\frac{\tau^{(1)}(x)}{h(x)}. \tag{18}$$

4.1.4 Considering $O(\delta^2)$ Terms

The second order corrections are the next set of non-trivial solutions although they increase considerably in complexity due to the forcing terms of the leading order. Due to this complexity they do not provide much additional insight into the system but do introduce y dependence in the pressure, longitudinal stress and horizontal velocity terms as well as quadratic y dependence in shear and vertical velocity.

4.2 Applying Friction Models

Having now determined the equations for the velocities, stresses and flow parameter given an arbitrary friction model, it is now straight forward to substitute a friction models to compare their behaviour and limitations.

4.2.1 Coulomb

Nondimensionalising the coulomb friction boundary condition gives

$$\tau = \frac{\mu}{\beta\delta}\left(p - s_{yy}\right)\frac{\Delta\mathbf{u}}{|\Delta\mathbf{u}|}.$$

This suggests $\beta = \frac{\mu}{\delta}$ which leaves the ordinary differential equation

$$\frac{dp^{(0)}}{dx} - \gamma\frac{\mu}{h(x)}p^{(0)}(x) = \frac{\gamma}{h(x)} + \frac{2}{\beta h(x)}\frac{dh}{dx}$$

due to the coupling between shear and pressure, where

$$\gamma = \begin{cases} 1 & : x < x_n \\ -1 & : x \geq x_n \end{cases}$$

This can be solved in each piecewise region for

$$p^{(0)} = e^{\int \mu\frac{\gamma(x)}{h(x)}dx}\left(c_0 + \int e^{-\int \mu\frac{\gamma(x)}{h(x)}dx}\frac{2}{\mu\gamma(x)}\frac{dh(x)}{dx}dx\right) - \frac{1}{\mu}.$$

where c_0 is a also a piecewise constant, constant either side of the neutral point. Assuming the parabolic form for the rollers, eq. (10), this can be simplified to

$$p^{(0)} = \left(\frac{x - 1 - \sqrt{\frac{r-1}{r}}}{x - 1 + \sqrt{\frac{r-1}{r}}}\right)^{\frac{\mu\gamma}{2}\sqrt{\frac{r}{r-1}}}\left(c_0 + \int\left(\frac{x - 1 + \sqrt{\frac{r-1}{r}}}{x - 1 - \sqrt{\frac{r-1}{r}}}\right)^{\frac{\mu\gamma}{2}\sqrt{\frac{r}{r-1}}}\frac{4r\left(x-1\right)}{\mu\gamma}dx\right) - \frac{1}{\mu}.$$

This result substitutes easily to complete the leading order shear stress

$$s_{xy}{}^{(0)} = y\left(\mu\frac{p^{(0)}(x) + 1}{h(x)} + \frac{2}{\beta h(x)}\frac{dh}{dx}\right).$$

As there is no first order correction to traction the first order correction to both pressure and shear stress are also found to be zero.

The velocity scaling and neutral point are determined by setting the coefficient for each piecewise region such that both end conditions are satisfied,

$$2\int_0^1 \sigma_{xx}(0, y)dy = T_{\text{in}}$$
$$2\int_0^{h(1)} \sigma_{xx}(1, y)dy = T_{\text{out}}.$$

The neutral point is then selected to ensure pressure continuity. This provides a roll speed relative to the workpiece where both can be determined by the workpiece entrance velocity or the roll speed, whichever is specified.

4.2.2 Relative-Slip

Repeating this for the relative-slip friction model, which is nondimensionalised as

$$\tau = \frac{\hat{\kappa}\Delta\hat{u}_0}{\beta\delta\hat{k}}\Delta u$$

where $\Delta\hat{u}_0 = \hat{U} - \hat{u}_0$ and $\hat{U}$ is the roll velocity. This would suggest $\beta = \frac{\hat{\kappa}\Delta\hat{u}_0}{\delta\hat{k}}$. With this, the pressure can be solved with a single integration,

$$p^{(0)} = \int \kappa\frac{U - u^{(0)}}{h(x)} + \frac{2}{\beta h(x)}\frac{dh}{dx}\,\mathrm{d}x,$$

which can be reduced to closed form with the rolls taking a parabolic form,

$$p^{(0)} = \frac{\kappa}{2}(U-r)\sqrt{\frac{r}{r-1}}\log\left(\frac{x-1-\sqrt{\frac{r-1}{r}}}{x-1+\sqrt{\frac{r-1}{r}}}\right) + \left(\kappa r + \frac{2}{\beta}\right)\log\left(1-r\left(2x-x^2\right)\right)$$

The shear is, again, an easy substitution for the closed form solution,

$$s_{xy}{}^{(0)} = y\left(\kappa\frac{U-u^{(0)}}{\Delta U h(x)} + \frac{2}{\beta h(x)}\frac{dh}{dx}\right).$$

4.3 Results

To first order the deviatoric longitudinal stresses are straight forward. The pressure and shear terms, however, exhibit the leading dynamics of rolling. It is evident from fig. 6 that both friction models exhibit the pressure hill although the neutral point is not coherent between the two models.

Both show zero shear along the centreline as prescribed by the boundary condition but the roll boundary has considerably different behaviour. The fault of each is the existence of a discontinuity: the Coulomb model is across the neutral point where the relative slip friction is maximal at the entrance and exit which transitions to a stress free boundary beyond the roll gap. It is likely this behaviour that motivated transition models like those described in section 3.1.3.

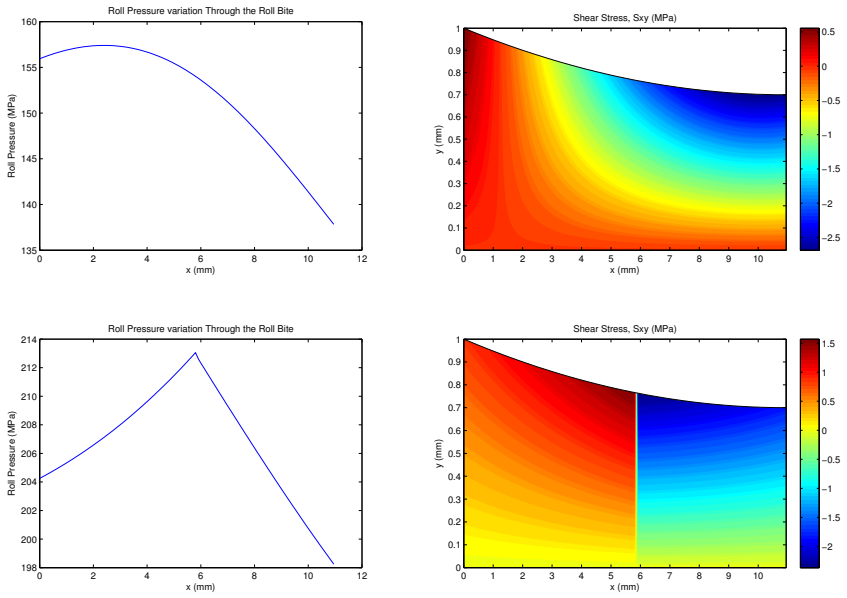

Figure 6: Plots showing the shear stress and pressure hill along the centreline for low magnitude relative-slip and Coulomb friction asymptotic models.

Both asymptotic models produce similar trends as the slab model and Orowan's model as the roll gap ratio, δ, is varied, although both force and torque result in higher estimates. This is also true for the relative-slip model as the friction coefficient is varied, however, the Coulomb friction model produces much higher values as the friction coefficient is increased. This is evident in fig. 7.

These results were compared to FE simulation, also included in fig. 7, generated by *ABAQUS* which is a commercial package. The parameters were matched as closely as possible wherever possible however an approximation for elasticity had to be made: the Young's modulus was turned up as high as was stable. The package also implements a Coulomb friction model. The results of the simulation do not appear to have converged so, although it is possible to find values that match well, this must be further investigated.

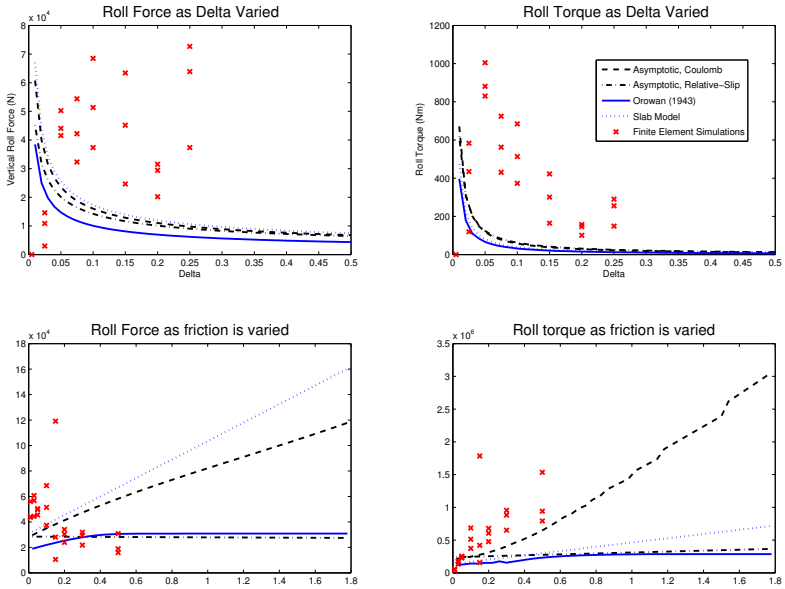

Figure 7: A comparison of roll force and torque values between finite element simulation, slab model, Orowan's solution and asymptotic models as the magnitude of friction and roll gap ratio varies.

4.4 Medium Friction

The solution process above can be repeated with $\bar{\beta} = O(1)$. This produces much the same results except the longitudinal deviatoric stress which, from eq. (7), takes the form

$$s_{xx}{}^{(0)} = -s_{yy}{}^{(0)} = \sqrt{1 - \bar{\beta}^2 s_{xy}{}^{(0)2}}$$

These equations can be solved for the relative-slip friction model and produce results that are similar to those of small friction. The longitudinal deviatoric stress is no longer homogeneous, however, the remaining variables are only altered by a scaling. In fig. 8 the maximum pressure and neutral points vary slightly from the small friction case.

The second challenge arises when friction and pressure are coupled such as the Coulomb friction model. The smallest order works satisfactorily, however, the larger orders require higher friction which is violated without compression end condition to raise the pressure in the roll gap. This is an inherent problem with the scaling used in Domanti et al. [1994] although it is not discussed there.

4.5 Discussion

Irrespective of the friction model the assumption of β becomes significant to the solution and at least three regimes must be solved for each material and friction combination pair to gain a complete understanding: $\beta = O(\delta)$, $\beta = O(1)$ and $\beta = O(\delta^{-1})$. This still does not account for high friction regimes transitioning to sticking, although, this can be circumnavigated by choosing a strain-rate hardening material model as the material will simply harden with increased shear. This is how Cherukuri et al. [1997] progressed through the friction regimes without addressing the issue of sticking.

Ultimately, this set of non-dimensional equations are solved differently depending on which friction model, material model and magnitude of friction is chosen. The common model choices are laid out with publications that address each combination in table 1.

Additional simplifications can also be made, such as small reductions, that can extend closed-form solutions to higher orders.

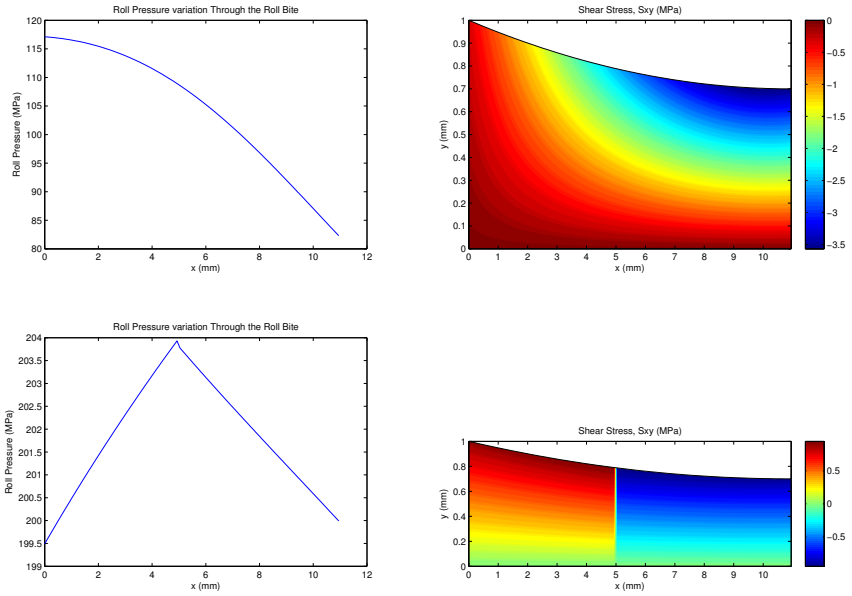

Figure 8: Shear stress and pressure distribution along the centreline for medium magnitude relative-slip and Coulomb friction asymptotic models.

Material Model	Coulomb Friction	Relative-Slip	No-Slip
Perfectly-Plastic	Domanti et al. [1994] This work	This work	
Strain-Rate Dependent		Cherukuri et al. [1997]	Cherukuri et al. [1997]
Strain Dependent	Smet and Johnson [1989]		

Table 1: Table of work performed on each material and friction models.

5 Weakly Asymmetric Friction, Geometry and Roll Speeds

In this section it is no longer assumed that the rolling process is symmetric; there may be variation between the top and bottom rolls in friction, size or drive speed. It is, however, assumed that for each of these characteristics the ratio between the top and bottom roll is of $O(1)$. The approach to finding a solution is identical to the previous section, except that integrals are taken between top and bottom roll surfaces instead of using the symmetry plane. This requires a second set of boundary conditions for which the parameters determining size, friction and roll speeds can be varied. The scalings used are the same as those in section 4.1 for the small β and the governing equations are the same as section 3 so this section proceeds straight to the solution for Coulomb and Relative-Slip frictions after briefly describing the assumed geometry.

5.1 Workpiece Alignment

Firstly, we take the rolls to be vertically aligned. It is then assumed that the workpiece feeds into the roll gap in such a way that the initial contact, tri-junction, with each roll, points A and B in fig. 9, are vertically aligned. The effect of plastic deformation will also ensure that the workpiece leaves the roll gap at the centre line of the rolls, where the roll bite is thinnest.

Asymmetry, in general, will induce a bending moment at either end of the roll bite, bending the workpiece around either roll and violating the previous assumptions about vertically aligned tri-junctions. This effect, however, is assumed to be negligible.

Defining roll sizes, R_t and R_b; total reduction, $2r = \frac{\Delta\hat{h}_t + \Delta\hat{h}_b}{2\hat{h}_0}$; and workpiece thickness $2\hat{h}_0$ is sufficient

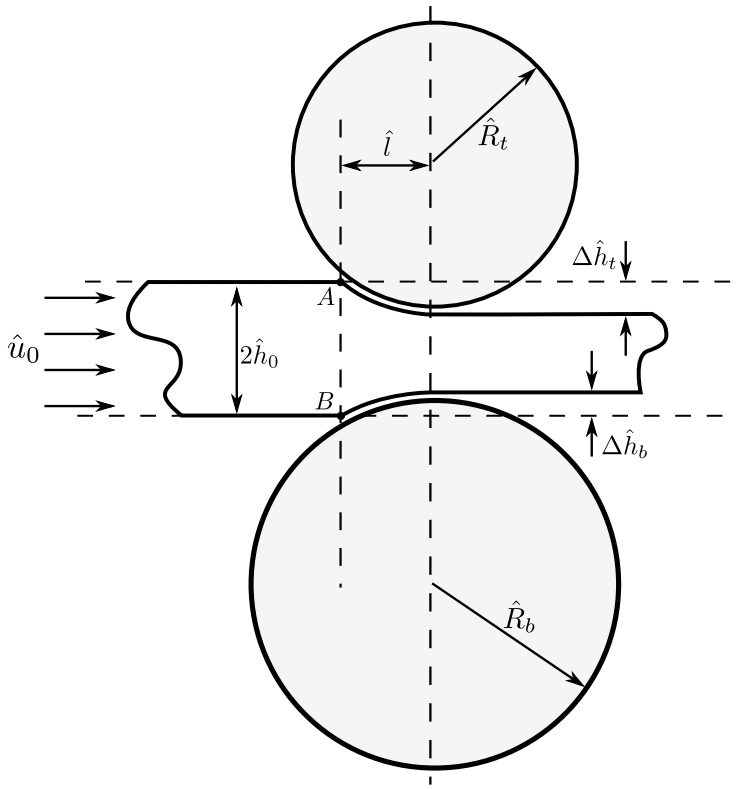

Figure 9: Illustration of the asymmetric roll configuration. Note the vertical alignment of tri-junctions, A and B, on the inlet. The same alignment for the outlet is required by vertically aligning the rolls.

to geometrically determine the system. It can then be calculated that the top and bottom reductions are given by

$$r_t = \frac{4r\hat{R}_b - 4r^2}{2\hat{R}_t + 2\hat{R}_b - 4r}$$
$$r_b = \frac{4r\hat{R}_t - 4r^2}{2\hat{R}_t + 2\hat{R}_b - 4r} = 2r - r_t$$

and the roll bite length is

$$\hat{l}^2 = \min\left(2\hat{R}\hat{h}_0 r - \hat{h}_0^2 r^2\right)$$

where both top and bottom are considered.

5.2 Coulomb Friction

Noting, for clarity, the top and bottom boundary conditions for shear are

$$s_{xy}(x,h_t) = \tau_t(x)\left(1+\delta^2\left(\frac{dh_t}{dx}\right)^2\right) - \frac{2}{\beta}\frac{dh_t}{dx}s_{yy}(x,h_t(x)) + \delta^2 s_{xy}(x,h_t(x))\left(\frac{dh_t}{dx}\right)^2 \tag{19}$$

$$s_{xy}(x,h_b) = \tau_b(x)\left(1+\delta^2\left(\frac{dh_b}{dx}\right)^2\right) - \frac{2}{\beta}\frac{dh_b}{dx}s_{yy}(x,h_b(x)) + \delta^2 s_{xy}(x,h_b(x))\left(\frac{dh_b}{dx}\right)^2 \tag{20}$$

and velocity

$$v(x,h_t) = \delta u(x,h_t)\frac{dh_t}{dx} \tag{21}$$

$$v(x,h_b) = \delta u(x,h_b)\frac{dh_b}{dx}. \tag{22}$$

Define $\Delta h = h_t(x) - h_b(x)$ for convenience.

Velocity is found to be

$$v^{(0)} = \frac{2}{\Delta h^2}\left(h_t\frac{dh_b}{dx} - h_b\frac{dh_t}{dx} + y\frac{d\Delta h}{dx}\right) \tag{23}$$

$$\text{and} \quad u^{(0)} = \frac{2}{\Delta h}. \tag{24}$$

Longitudinal deviatoric stress required no integration and so is found to be the same.
The flow parameter can now be solved for

$$\lambda^{(0)} = \frac{2}{\Delta h^2}\frac{d\Delta h}{dx}. \tag{25}$$

This leaves the pressure and shear stress which can be solved in their general form as

$${s_{xy}}^{(0)} = \frac{s_{xy}^{(0)}(x,h_t(x)) - s_{xy}^{(0)}(x,h_b(x))}{h_t(x)-h_b(x)}y + \frac{h_t(x){s_{xy}}^{(0)}(x,h_b(x)) - h_b(x){s_{xy}}^{(0)}(x,h_t(x))}{h_t(x)-h_b(x)}. \tag{26}$$

and

$$\frac{dp^{(0)}}{dx} = \frac{{s_{xy}}^{(0)}(x,h_t(x)) - {s_{xy}}^{(0)}(x,h_b(x))}{h_t(x)-h_b(x)} \tag{27}$$

where the constant of integration are to be solved, as discussed before, using the end tensions.

For a Coulomb friction model, the boundary shear terms would be

$$\tau_t = \gamma_t\boldsymbol{\sigma}(x,h_t(x))\cdot\mathbf{n} = \gamma_t\left(\beta p(x,h_t) + s_{xx}(x,h_t) + \delta^2\left(2\beta\sigma_{xy}(x,h_t)\frac{dh_t}{dx} - 2s_{xx}(x,h_t)\right)\left(\frac{dh_t}{dx}\right)^2 + O\left(\delta^4\right)\right) \tag{28}$$

$$\tau_b = \gamma_b\boldsymbol{\sigma}(x,h_b(x))\cdot\mathbf{n} = \gamma_b\left(\beta p(x,h_t) + s_{xx}(x,h_b) + \delta^2\left(2\beta\sigma_{xy}(x,h_b)\frac{dh_b}{dx} - 2s_{xx}(x,h_b)\right)\left(\frac{dh_b}{dx}\right)^2 + O\left(\delta^4\right)\right) \tag{29}$$

where

$$\gamma_t = \begin{cases} 1 & : x < x_{nt} \\ -1 & : x > x_{nt} \end{cases}, \qquad \gamma_b = \begin{cases} -\frac{\mu_b}{\mu_t} & : x < x_{nb} \\ \frac{\mu_b}{\mu_t} & : x > x_{nb} \end{cases}, \tag{30}$$

and x_{nt} is the neutral point on the top roller and x_{nb} is the equivalent on the bottom roller. This introduces a third region to the piecewise function of pressure, known as the region of cross shear.

Define $\Delta\gamma = \gamma_t - \gamma_b$. Like in the symmetric case, the differential equation for pressure is solved in each of the three regions where $\Delta\gamma$ is constant and then each solution is matched at the steps.

Two are found by matching coefficients at the entrance and exit of the roll gap. The last, by the intersection with the previous two, determine the two neutral points which in turn determines the roll velocities. This choice must therefore must satisfy the specified roll speed ratio such that $\frac{u^{(0)}(x_{Nt})}{u^{(0)}(x_{Nb})} = \frac{U_t}{U_b}$. This coupling is illustrated in fig. 10. The absolute velocities are then satisfied by changing the velocity scaling of the solution, $\hat{u}_0$.

Making the substitution produces the differential equation, having gained a term from the symmetric case,

$$\frac{\partial p^{(0)}}{\partial x} - \beta p^{(0)}\frac{\Delta\gamma}{\Delta h} = \frac{\Delta\gamma}{\Delta h} + \frac{2}{\beta\Delta h}\frac{d\Delta h}{dx}.$$

If $\Delta\gamma = 0$ then

$$p^{(0)} = \frac{2}{\beta}\log\left(\Delta h\right) + c_0$$

and if $\Delta\gamma \neq 0$ then

$$p^{(0)} = e^{\int\beta\frac{\Delta\gamma}{\Delta h}dx}\left(c_0 + \int e^{-\int\beta\frac{\Delta\gamma}{\Delta h}dx}\frac{2}{\beta\Delta\gamma}\frac{d\Delta h}{dx}dx\right) - \frac{1}{\beta}.$$

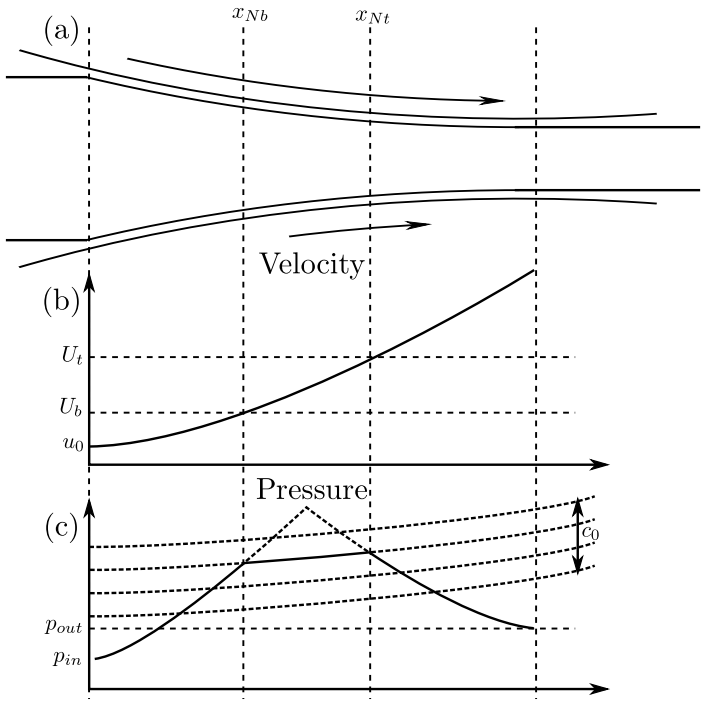

Figure 10: Figure showing the qualitative form of the sections of pressure.

After substituting parabolic rollers and assuming $\Delta\gamma$ is constant over the considered range,

$$p^{(0)} = \left(\frac{x-1-\sqrt{\frac{r-1}{r}}}{x-1+\sqrt{\frac{r-1}{r}}}\right)^{\beta\frac{\Delta\gamma}{2}\sqrt{\frac{r}{r-1}}} \left(c_0 + \int \left(\frac{x-1+\sqrt{\frac{r-1}{r}}}{x-1-\sqrt{\frac{r-1}{r}}}\right)^{\beta\frac{\Delta\gamma}{2}\sqrt{\frac{r}{r-1}}} \frac{4r\,(x-1)}{\beta\Delta\gamma} dx\right) - \frac{1}{\beta}.$$

Note that a closed form of this integral can be produced using hypergeometric and Appell hypergeometric functions.

Now the shear stress can be determined by substituting this result into

$$s_{xy}{}^{(0)}(x,y) = -\frac{\beta p^{(0)}(x)+1}{\Delta h}\left(\Delta\gamma y + (\gamma_t(x)h_b(x) - \gamma_b(x)h_t(x))\right).$$

Like the symmetric case, there is no contribution by the first order correction.

$O(\delta^2)$ terms increase in complexity again due to the difference in terms presented in this section. They are still solvable.

5.3 Relative-Slip Friction

Up to $O(1)$ both solutions match except for the leading order pressure and shear. The tractions becomes

$$\tau_t = \frac{U_t - u_s(x,h_t(x))}{\Delta U} = \frac{U_t - u(x,h_t(x))\left(1+\frac{1}{2}\delta^2\frac{d^2h}{dx^2}+O(\delta^3)\right)}{U_t-u_0} \tag{31}$$

$$\tau_b = \kappa\frac{U_b - u_s(x,h_b(x))}{\Delta U} = -\kappa\frac{U_b - u(x,h_b(x))\left(1+\frac{1}{2}\delta^2\frac{d^2h}{dx^2}+O(\delta^3)\right)}{U_b-u_0} \tag{32}$$

which gives shear as

$$s_{xy}{}^{(0)}(x,h_t(x)) = \frac{u^{(0)}(x,h_t(x))-U_t}{\Delta U} - \frac{2}{\beta}\frac{dh_t}{dx} = \frac{2-U_t\Delta h}{\Delta h\Delta U} - \frac{2}{\beta}\frac{dh_t}{dx} \tag{33}$$

$$\text{and}\quad s_{xy}{}^{(0)}(x,h_b(x)) = -\kappa\frac{u^{(0)}(x,h_b(x))-U_b}{\Delta U} - \frac{2}{\beta}\frac{dh_b}{dx} = -\kappa\frac{2-U_b\Delta h}{\Delta h\Delta U} - \frac{2}{\beta}\frac{dh_t}{dx}. \tag{34}$$

The pressure term can now be integrated directly.

5.4 Results and Discussion

Unsurprisingly, the results of the asymmetric solution are very similar to the symmetric case. Asymmetric friction coefficients have the most subtle effect: moving the line of zero shear toward the roll with less friction and moving the neutral point in the relative-slip model. Roll sizes have a similar effect by moving the line of zero shear toward the smaller roll and drifting the neutral point in the relative-slip model. Both these trends can be made out comparing fig. 11 or fig. 12 with the earlier plots, fig. 6.

Asymmetric roll speed has the biggest impact as it directly moves one of the neutral points. This occurs in both models, particularly relevant for the Coulomb model as this region of cross shear has distinctly different behaviour as a region of more constant shear through the sheet thickness. This is marked by the large red zone in fig. 11.

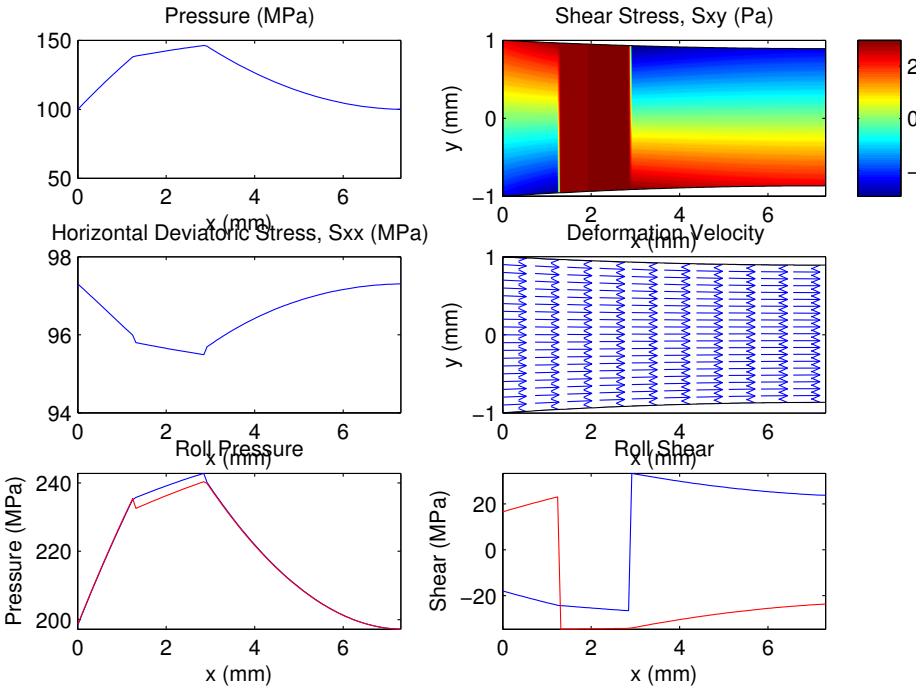

Figure 11: Pressure, shear stress, deviatoric stress, flow map, roll pressure and roll shear for a asymmetric small Coulomb friction asymptotic model.

Section 5.4 presents the force and torque for each roll of the Coulomb friction model as the indicated value of the bottom roll is varied. In comparison to finite element results, these models do not match closely in magnitude or trend.

The results in section 5.4 are after $\Delta\gamma$ is taken as $\mu_b - \mu_t$ instead of $1 - \mu_t/\mu_b$.

This ad-hoc adjustment appears to be sufficient to match the trends in force and torque while the roll speeds change. This also requires more investigation as it may be the result of a subtlety of taking exponentials of a small parameters.

6 Future Work

Thus far models have been developed for both symmetric and weakly asymmetric rolling in a thin-sheet and low friction regime. Further work is required to validate each of these models.

Producing a numerical solver to solve the exact governing equations is the next step to validate the correctness of the asymptotic models and to provide some quantification of the error as each parameter is varied.

Finding a steady state FE solution for the rolling problem would also provide evidence for the correctness of the asymptotics but alternatively may highlight phenomena that are not captured by the model such as the significance of elasticity and hardening.

After the completion of the rolling machine, or a collaboration with another laboratory such as that from the University of Aachen, experimental comparison would provide scope for a quantitative review

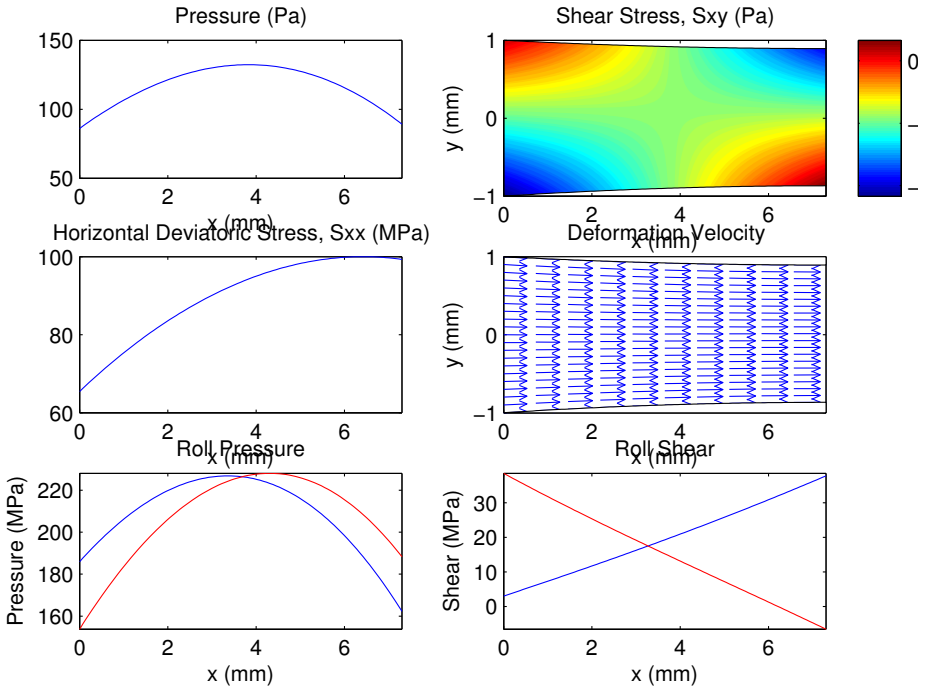

Figure 12: Pressure, shear stress, deviatoric stress, flow map, roll pressure and roll shear for a asymmetric small relative-slip friction asymptotic model.

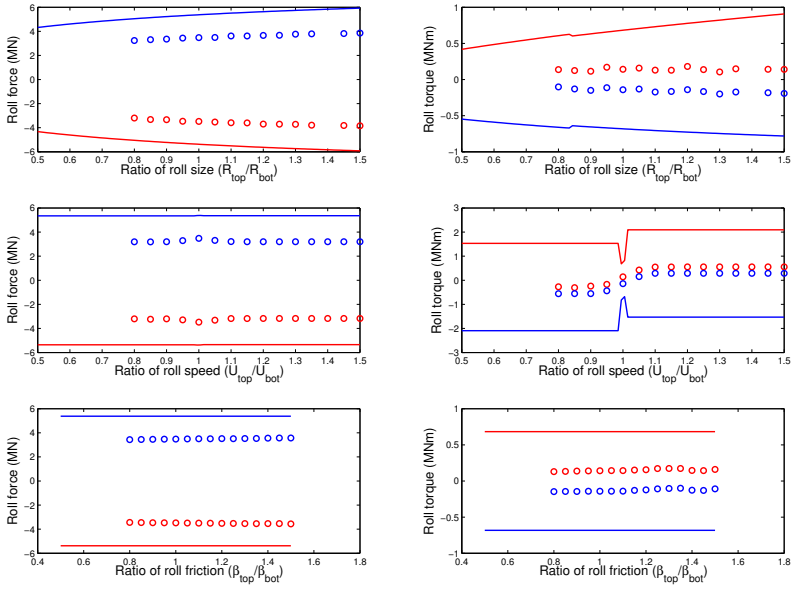

Figure 13: Comparison of roll force and torque between small Coulomb friction, asymmetric asymptotic model and FE simulations as roll size, speed and friction ratios are varied. The ratio is determined by holding the top roll constant and varying the parameter of the bottom roll only.

of the models available in literature. This may be enhanced by completing additional rows or columns of table 1 to compare the impact and significance of material and friction models.

Many opportunities also exist to incorporate more complex physics and phenomena into the models.

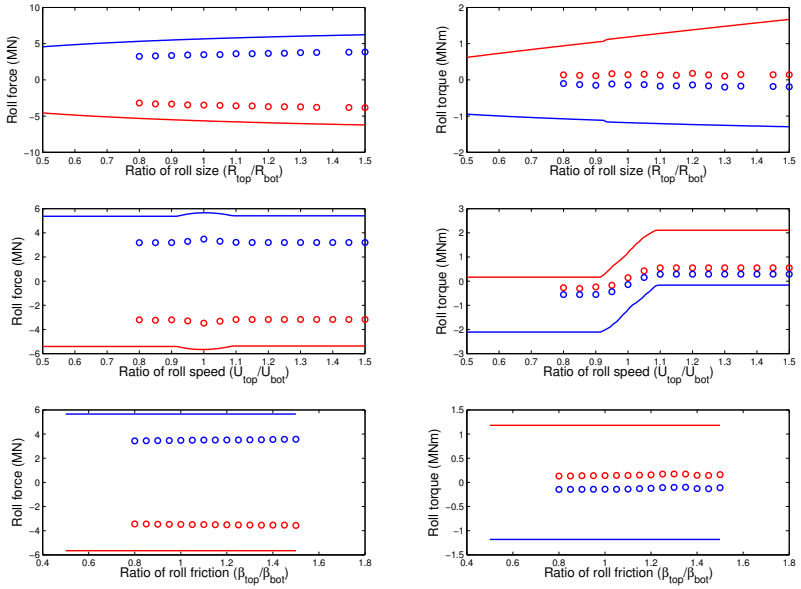

Figure 14: Comparison of roll force and torque between small Coulomb friction, asymmetric asymptotic model with a fudge to the exponential pressure term and FE simulations as roll size, speed and friction ratios are varied. The ratio is determined by holding the top roll constant and varying the parameter of the bottom roll only.

6.0.1 Moments and Curvature

A brief investigation was carried out to vary the boundary by parameterising an additional point and create a triangular shape, this is illustrated in section 6.0.1 where the two parameters are a and b. Three values define the boundary condition: a, b and $\int \hat{\sigma}_{xx}(0, y)dy$. Two valid conditions are found to determine these values in the horizontal force and bending moment, however, the vertical force is identically zero. This means small bending moments could be supported but the boundary apex would only be restricted to a curve of solutions.

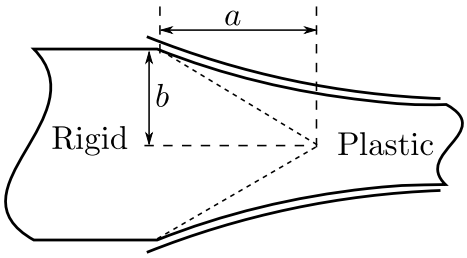

Figure 15: Illustration of a non-square plastic region within the roll gap parameterised by a and b.

Limitations to this investigation are probably due to the necessity of elasticity and the movement of the trijunction to match a general boundary condition. Asymmetric rolling produces moments on the worked and unworked sections of the sheet but it unclear whether this alone is sufficient to account for the bending that occurs in regular operation or processes like ring rolling.

6.0.2 Coupling Additional Physics

Roller deformation is also a major concern for the regime these models are relevant in: cold, thin-sheet rolling. There is a possibility to incorporate a simple elastic roller model into the asymptotic analysis.

Temperature would be another interesting addition to the model, however, this is likely a challenging proposition. Temperature is tightly coupled with plastic deformation through dependencies of the

material properties on temperature and heating effects from deformation energy.

6.1 Other Processes

6.1.1 Ring Rolling

Two major challenges exist in modelling ring rolling. The first is the significant moments that act as boundary conditions to the roll gap. These are coupled entry to exit by an outer problem of the ring elasticity. The second is the aspect ratio of rings are often much thicker than the regimes presented here; as much ten times thicker than longer. This may be sufficiently thick to utilise a boundary-layer approach to model the effect of the rolls and using a matched asymptotic expansion find a sufficiently broad technique to cover the entire operating regime.

Using an alternative approximate, empirical or even numerical solution to the inner problem may also lead to some useful results such as stability conditions when matched to the outer problem.

6.1.2 English Wheel

Another exciting modelling application is the English wheel. It is an application that exists closer to the small aspect ratio regime but requires the extension to three dimensions. Ensuring compatibility span-wise will require some consideration of elastic effects but similar to the ring rolling model, other solution methods could to match to an outer solution.

The outer solution would be a shell model to calculate compatibility through an out of plane deformation of the plate. This may be sufficient to generate a work path for process automation. No solution currently exists in literature for this.

References

J.M. Alexander. A Slip Line Field for the Hot Rolling Process. *Proceedings of the Institution of Mechanical Engineers*, 169:1021, 1955. doi: 10.1243/PIME.

J.M. Alexander. On the Theory of Rolling. *Proceedings of the Royal Society A: Mathematical, Physical and Engineering Sciences*, 326(1567):535–563, February 1972. ISSN 1364-5021. doi: 10.1098/rspa.1972.0025. URL `http://rspa.royalsocietypublishing.org/cgi/doi/10.1098/rspa.1972.0025`.

D. R. Bland and Hugh Ford. The calculation of roll force and torque in cold strip rolling with tensions. *Proceedings of the Institution of Mechanical Engineers*, 159:144, June 1948a. doi: 10.1243/PIME. URL `http://pme.sagepub.com/content/159/1/144.short`.

D.R. Bland and H. Ford. An approximate treatment of the elastic compression of the strip in cold rolling. *Journal of Iron Steel Institute*, 171:245–249, 1948b.

S. A. E. Buxton and S. C. Browning. Turn-up and Turn-down in Hot Rolling: A Study on a Model Mill Using Plasticine. *Journal of Mechanical Engineering Science*, 14(4):245–254, 1972. doi: 10.1243/JMES.

A. P. Chekmarev and A.A. Nefedov. No Title. *Obrabotka Metallov Davleniem*, 4:2–15, 1956. URL `(British Library Translation R.T.S. 8939)`.

H.P. Cherukuri, Robert E. Johnson, and R.E. Smelser. A Rate-Dependent Model for Hot-Rolling. *International Journal of Mechanical Sciences*, 39(6):705–727, 1997.

Ian F. Collins. Slipline Field Solutions for Compression and Rolling with Slipping Friction. *International Journal of Mechanical Sciences*, 11:971–978, 1969.

Ian F. Collins and P. Dewhurst. A Slipline Field Analysis of Asymmetrical Hot Rolling. *International Journal of Mechanical Sciences*, 17:643–651, 1975.

S.A. Dassault Systemes. Abaqus 6.12 Example Problems Manual, 2012.

P. Dewhurst, I.F. Collins, and W. Johnson. A theoretical and experimental investigation into asymmetrical hot rolling. *International Journal of Mechanical Sciences*, 16(6):389–397, June 1974. ISSN 00207403.

S.A. Domanti and D. L. S. McElwain. Two-Dimensional Plane Strain Rolling: An Asymptotic Approach to the Estimation of Inhomogeneous Effects. *International Journal of Mechanical Sciences*, 37(2): 175–196, 1995.

S.A. Domanti and D.L.S. McElwain. Cold rolling of flat metal products: contribution of mathematical modelling. *Proceedings of the Institution of Mechanical Engineers, Part B: Journal of Engineering Manufacture*, 212(1):73–86, January 1998. ISSN 0954-4054. doi: 10.1243/0954405981515518. URL `http://pib.sagepub.com/lookup/doi/10.1243/0954405981515518`.

S.A. Domanti, D.L.S. McElwain, and R.H. Middleton. Model of cold rolling of thin metal sheets between nonparallel rolls. 18(July), 1994.

M. I. Ghobrial. A Photoelastic Investigation on the Contact Stresses Developed in Rolls During Asymmetrical Flat Rolling. *International Journal of Mechanical Sciences*, 31(10):751–764, 1989.

R.M. Govindarajan and N Aravas. Asymptotic Analysis of Extrusion of Porous Metals. *Journal of Mechanical Science*, 33(7):505–527, 1991.

P. Hartley, C.E.N Sturgess, C. Liu, and G.W. Rowe. Experimental and Theoretical Studies of Workpiece Deformation, Stress, and Strain During Flat Rolling. *International Materials Reviews*, 34(1):19–34, 1989.

Yeong-Maw Hwang and Gow-Yi Tzou. An Analytical Approach to Asymmetrical Cold- and Hot-Rolling of Clad Sheet Using the Slab Method. *Journal of Materials Processing Technology*, 62:249–259, 1996.

Robert E. Johnson. Conical extrusion of a work-hardening material: an asymptotic analysis. *Journal of Engineering Mathematics*, 21(4):295–329, 1987. ISSN 0022-0833. doi: 10.1007/BF00132681. URL `http://link.springer.com/10.1007/BF00132681`.

Robert E. Johnson. Shape Forming and Lateral Spread in Sheet Rolling. 33(6):449–469, 1991.

Robert E. Johnson. The Effect of Friction and Inelastic Deformation on Chatter in Sheet Rolling. *Proceedings of the Royal Society A: Mathematical, Physical and Engineering Sciences*, 445(1925):479–499, June 1994a. ISSN 1364-5021. doi: 10.1098/rspa.1994.0073. URL `http://rspa.royalsocietypublishing.org/cgi/doi/10.1098/rspa.1994.0073`.

Robert E. Johnson. Cold Sheet Rolling with Unequal Friction at the Roll-Sheet Interfaces. In *Manufacturing Science and Engineering*, volume 68, pages 619–626, 1994b.

Robert E. Johnson and R.G. Keanini. An asymptotic model of work roll heat transfer in strip rolling. *International Journal of Mass Transfer*, 41:871–879, 1998.

Robert E. Johnson and R.E. Smelser. An asymptotic formulation of shear effects in two dimensional rolling. *Journal of Materials Processing Technology*, 34:311–318, 1992.

W. Johnson and G. I. Needham. Further Experiments in Asymmetrical Rolling. *International Journal of Mechanical Sciences*, 8:443–455, June 1966.

M.E. Karabin and R.E. Smelser. A quasi-three-dimensional analysis of the deformation processing of sheets with applications. *International Journal of Mechanical Sciences*, 32(5): 375–389, January 1990. ISSN 00207403. doi: 10.1016/0020-7403(90)90167-H. URL `http://linkinghub.elsevier.com/retrieve/pii/002074039090167H`.

T.von Karman. Zeit.Ang. *Zeitschrift fur angewandte Mathematik und Mechanik*, 5:142, 1925.

G.E. Kennedy and F. Slamar. Turn-up and Turn-down in Hot Rolling. *Iron and Steel Engineer*, 35:71, 1958.

M. M. Kiuchi and S. Hsiang. Analytical Model of Asymmetrical Rolling Process of Sheets. *Proceedings of the 14th NAMRC, Society of Manufacturing Engineers, Minneapolis*, page 384, 1986.

C. W. Knight, S. J. Hardy, A. W. Lees, and K. J. Brown. Influence of roll speed mismatch on strip curvature during the roughing stages of a hot rolling mill. *Journal of Materials Processing Technology*, 168(1):184–188, September 2005. ISSN 09240136.

T.A.M. Langlands and D.L.S. McElwain. A modifed Hertzian foil rolling model : approximations based on perturbation methods. 44:1715–1730, 2002.

Jerzy Mischke. Equations of Strip Equilibrium During Asymmetrical Flat Rolling. *Journal of Materials Processing Technology*, 61:382–394, 1996.

Pierre Montmitonnet. Hot and cold strip rolling processes. *Computer Methods in Applied Mechanics and Engineering*, 195(48-49):6604–6625, October 2006. ISSN 00457825. doi: 10.1016/j.cma.2005.10.014. URL `http://linkinghub.elsevier.com/retrieve/pii/S0045782505004779`.

Pierre Montmitonnet and P. Buessler. A Review on Theoretical Analyses of Rolling in Europe. 31(6): 525–538, 1991.

A. Nadai. "Plasticity". *Journal of Applied Mechanics1*, 6:A–55, 1931.

E Orowan. The calculation of roll pressure in hot and cold flat rolling. *Proceedings of the Institution of Mechanical Engineers*, 150:140–167, July 1943. ISSN 0020-3483. doi: 10.1243/PIME_PROC_1943_150_025_02. URL `http://pme.sagepub.com/lookup/doi/10.1243/PIME_PROC_1943_150_025_02`.

E Orowan and K.J. Pascoe. *First Report of the Rolling-Mill Research Sub-Committee*. Iron and Steel Institute, London, 1946.

D. Pan and D. H. Sansome. An Experimental Study of the Effect of Roll-Speed Mismatch on the Rolling Load During the Cold Rolling of Thin Strip. *Journal of Mechanical Working Technology*, 6:361–377, 1982.

Ann Bettina Richelsen. Elastic-Plastic Analysis of the Stress and Strain Distributions in Asymmetric Rolling. *International Journal of Mechanical Sciences*, 39(11):1199–1211, 1997.

G Sachs and L. J. Klinger. The Flow of Metals through Tools of Circular Contour. *Trans. ASME, Journal of Applied Mechanics*, 69:88–98, 1947.

M. Salimi and F. Sassani. Modified slab analysis of asymmetrical plate rolling. *International Journal of Mechanical Sciences*, 44:1999–2023, 2002.

R. Sauer and O. Pawelski. Theoretical study of the effect of asymmetries on the cold rolling process. *Steel Res.*, 58(7):319–326, 1987.

R. Shivpuri, P. C. Chou, and C. W. Lau. Finite Element Investigation of Curling in Non-Symmetric Rolling of Flat Stock. *International Journal of Mechanical Sciences*, 30(9):625–635, 1988.

E. Siebel. Berichte des Walzwerksausschusses. *Verein deutsher Eisenhuttenleute*, 37:1–4, 1924.

E. Siebel. Zur theories des walzvoganges bei ungleich angetriebenen walzen. *Archiv fur das Eisenhuettenwesen*, 15:125, 1941.

E. Siebel and A. Pomp. Mitteilungen aus dem Kaiser. *Mitteilungen aus dem Kaiser Wilhelm Institut fur Eisenforshung, Dussledorf*, 9:157, 1927.

Robert P Smet and Robert E. Johnson. An Asymptotic Analysis of Cold Sheet Rolling. *Journal of Applied Mechanics*, 56(March 1989):33–39, 1989.

R. D Venter and A Abd-Rabbo. Modelling of the Rolling Process I: Inhomogeneous Deformation Model. *International Journal of Mechanical Sciences*, 22(2):83–92, 1980.

R. D Venter and A Adb-Rabbo. Modelling of the Rolling Process II: Evaluation of the Stress Distribution in the Rolled Material. 22:93–98, 1980.